

Published in final edited form as:

Pacing Clin Electrophysiol. 2012 February ; 35(2): 204–214. doi:10.1111/j.1540-8159.2011.03243.x.

Biophysical Modelling to Simulate the Response to Multisite Left Ventricular Stimulation using a Quadripolar Pacing Lead

SA Niederer¹, AK Shetty^{1,2}, G Plank³, J Bostock², R Razavi^{1,2}, NP Smith^{1,4}, and CA Rinaldi^{1,2}

¹Imaging Sciences & Biomedical Engineering Division, King's College London

²Department of Cardiology, St Thomas' Hospital, London

³Institut für Biophysik, Medizinische Universität Graz

⁴Computing Laboratory, University of Oxford

Abstract

Background—Response to Cardiac Resynchronisation Therapy (CRT) is reduced in patients with postero-lateral scar. Multipolar pacing leads offer the ability to select desirable pacing sites and/or stimulate from multiple pacing sites concurrently using a single lead position. Despite this potential, the clinical evaluation and identification of metrics for optimisation of multisite CRT (MCRT) has not been performed.

Methods—The efficacy of MCRT via a quadripolar lead with two LV pacing sites in conjunction with RV pacing was compared with single site LV pacing using a coupled electro-mechanical biophysical model of the human heart with no, mild or severe scar in the LV postero-lateral wall.

Result—The maximum dp/dt_{max} improvement from baseline was 21%, 23%, 21% for standard CRT vs 22%, 24%, 25% for MCRT for no, mild and severe scar, respectively. In the presence of severe scar there was an incremental benefit of multisite vs standard CRT (25% vs 21%, 19% relative improvement). Minimizing total activation time (analogous to QRS duration) or minimizing the activation time of short axis slices of the heart did not correlate with CRT response. The peak electrical activation wave area in the LV corresponded with CRT response with an R^2 value between 0.42-0.75.

Conclusion—Biophysical modelling predicts that in the presence of postero-lateral scar MCRT offers an improved response over conventional CRT. Maximising the activation wave area in the LV had the most consistent correlation with CRT response, independent of pacing protocol, scar size or lead location.

Correspondence: Steven Niederer, Biomedical Engineering Department, The Rayne Institute, St Thomas' Hospital, London SE17EH, Ph.+44(0)2071885441, Fax.+44(0)2071885442, steven.niederer@kcl.ox.ac.uk.

Disclosures

Anoop Shetty receives a St Jude Medical educational grant and Christopher Rinaldi receives St Jude educational support and is on advisory boards for St Jude Medical and Medtronic.

Introduction

Cardiac resynchronization therapy (CRT) is an effective treatment for medically refractory patients with heart failure and left branch bundle block (1–3). Despite the mortality, morbidity and quality of life benefits, 30–40% of patients still fail to respond to CRT (4). One potential strategy to improve response is multisite left ventricular (LV) stimulation which has the capacity to produce simultaneous recruitment of a larger volume of viable myocardium and thus more effectively reverse dyssynchrony. While, multisite CRT (MCRT) has been previously applied using two separate LV pacing leads (5). New lead technologies allow multisite stimulation to be delivered through a single multipolar lead (6; 7).

Specifically, the cathodal programmability available with a quadripolar lead (Quartet LV lead model 1458Q, St Jude Medical, Sylmar, CA, USA) allows stimulation of the LV myocardium using multiple vectors. The 4 LV lead electrodes can act as cathodes and 2 as anodes and the RV coil can act as an anode giving 10 possible different pacing configurations. The lead has a 4.0 Fr tip and 4.7 Fr maximum body diameter with three ring electrodes (M2,M3,P4) located 20, 30, and 47 mm from the distal electrode (D1). The lead can be used in a conventional way for single site LV stimulation but the multiple vectors available have been shown to be useful in overcoming problems with phrenic nerve stimulation and high capture thresholds (6; 7). Additionally, this quadripolar lead has the ability to perform true multisite pacing of the LV using two different vectors with a minimum 5ms delay between them. With a RV electrode also used, this allows up to three ventricular sites to be paced at the same time, thus increasing the points of early activation in the heart.

Despite the options provided this quadripolar lead, it is important to note that, given the relative close proximity of the electrodes, increasing the number of pacing sites may not necessarily produce a significant improvement. Furthermore, the increased number of pacing sites and the corresponding increase in the temporal and spatial pacing combinations means that optimising such a device for a specific patient is a challenge in itself. The number of potential pacing permutations greatly limits the capacity to comprehensively evaluate all combinations or optimise the lead through trial and error in a single patient thus necessitating improved optimisation algorithms. The difficulty in both testing and validating such algorithms, is that while safety studies of multisite pacing are currently being performed, there is currently no clinical data on the hemodynamic effect of multisite stimulation using the quadripolar lead.

In-silico biophysical models allow the possibility to test multiple pacing parameters (8). To provide an initial prediction of the efficacy of multisite pacing with a quadripolar lead and to facilitate the proposal of optimisation algorithms we applied this approach to evaluate the effects of multisite pacing in a computational coupled electro-mechanical human heart model. The model simulates single or multisite LV pacing in conjunction with RV pacing and can be tested in the presence of no, moderate or severe LV transmural postero-lateral scar. These simulations predict the contractile ability of the heart for each pacing combination, measured using the maximum rate of pressure increase during ventricular systole (dP/dt_{max}), and provide a quantitative evaluation of the effects of MCRT compared

with conventional CRT. Using a complete set of pacing combinations we then evaluate three potential optimisation algorithms based on total activation time, cumulative fraction of activated volume and activation time of short axis slices, parallel to base (see Fig. 2).

Methods

Modelling Methods

The computational model is based on a coupled electro-mechanical human heart model developed previously (8) using invasive data from a 60-year-old female with NYHA Class III heart failure an LV ejection fraction of 25% and left bundle branch block (QRS duration of 154 ms). The mechanics and electrophysiology model were validated pre and post CRT against endocardial activation patterns derived from non-contact mapping (Ensite), MRI derived wall motion and pressure catheter measures. In this study two simplifying assumptions were made to reduce confounding factors. The heart was assumed to have no native activation and the myocardium was treated as homogenous.

Simulations were performed using the bi-domain approximation of myocardial electrical activation in the heart. Simulations were performed using CARP (9) (<http://carp.medunigraz.at>) on the UK National HPC resource HeCTOR (www.hector.ac.uk). The electrophysiology model had 35 million and 26 million extra and intra cellular degrees of freedom, respectively, 208 million elements and took ~3 hours to solve using 512 cores. Mechanics simulations were performed using CMISS (www.cmiss.org) on ORAC at the Oxford e-Research Centre (www.oerc.ox.ac.uk).

Pacing Model

To simulate pacing we manually aligned the coronary venous anatomy from steady state free precession (SSFP) MRI with the model geometry derived from cine MRI. The coronary venous anatomy provided the location for the quadripolar lead that was introduced into the model. RV septal and apical lead positions were introduced in the centre of the RV. All electrodes are shown in Fig. 1A. LV pacing was between the D1 (cathode) and M2 (anode) or M3 (cathode) and P4 (anode) electrodes. RV pacing was between the RV tip (cathode) in the septum or apex position and the RV coil (anode). Stimulation was simulated by raising the cathode electrode to 2V for 0.5ms and grounding the anode electrode.

Scar Model

Simulations were performed using the model with no scar or in the presence of a transmural basal LV postero-lateral scar with a 60 mm diameter, as shown in Fig. 1B. Scar was simulated by reducing conduction and decreasing anisotropy (10). Conduction velocities decrease by ~50% between viable tissue and scar (11). From the cable equation conduction velocity is proportional to the square route of conductivity (the inverse of resistance) (12). Hence scar was simulated by a 50% or a 90% decrease in the conductivity value corresponding to 30% or 70% decrease in conduction velocity, for mild and severe scar, respectively. The quadripolar lead was placed across the scar with the most distal pole D1 out of the scar, M2 on the scar border and M3 and P4 basally within the scar.

Cardiac function and efficacy of CRT

The efficacy of each pacing mode was evaluated using the change in dP/dt_{\max} as a metric of improvement. RV apical pacing dP/dt_{\max} was used as a baseline, as the model had no intrinsic activation. We normalised all CRT responses by dP/dt_{\max} calculated for an instantaneous homogenous activation pattern.

Simulations

For standard CRT (single LV stimulation site and RV stimulation) simulations were performed with the LV or RV site paced first with a 5, 15, 30 or 45ms delay. For MCRT (two LV pacing sites and one RV) the three stimulations were separated by two delays, one delay interval was always 5ms and the other delay interval was 5, 15, 30 or 45ms. The sites could be paced in any order except that the RV site had to be paced either before or after the LV pacing. Activation times for combinations of pacing sites were calculated by combining activation patterns from each individual site as described in the online supplement.

Optimisation Algorithms

QRS duration has been reported to correlate with CRT response (13–17) and provide an effective metric of asynchrony to identify CRT candidates (4). To test this hypothesis we compared CRT response with QRS duration, using total activation time of both ventricles as an analog of QRS duration. Previous studies have shown that pacing the LV only increased QRS duration, potentially due to late activation of the RV (18). To account for this effect we provide results for activation times, both for the combined LV and RV and for the LV alone.

If the bulk of the heart is rapidly and synchronously activated then late activation of peripheral regions that prolong QRS duration may confound relationships between QRS and CRT response. Maximising the peak rate of volume activation may minimize bulk activation asynchrony and lead to improved cardiac function. To test this hypothesis we calculated derivative of the cumulative activation curve and plotted this against CRT response.

The length dependence of cardiac muscle combined with the circumferential fibre direction in the mid LV wall means that effective LV contraction maybe achieved when a continuous strand of activated myocardium is formed around the circumference of the LV. When all myocardium is activated in such a loop the length dependence of the muscle will spatially regulate tension development so that during isovolumetric contraction muscle length is maintained allowing it to generate higher tension and hence improved dP/dt_{\max} . To test if activation loops in the LV correlate with dP/dt_{\max} in seven short axis slices we evaluated the time that the first loop of myocardium around the LV is activated, when the whole of the slice is activated in both the LV and RV and when the whole of the slice in the LV is activated.

Results

Baseline Results

Maximum dP/dt_{\max} was calculated for a homogenous instantaneous activation of the myocardium, resulting in a theoretical maximum dP/dt_{\max} of 1295 mmHg s^{-1} . Baseline

dP/dt_{\max} (RV apical pacing) was 906, 885 and 825 mmHg s⁻¹ for no, mild and severe scar or 0.7, 0.683 and 0.64 of the maximum value.

Single Site and Multisite LV stimulation

Figure 3 and 4 show the fraction of the theoretical maximum dP/dt_{\max} reached with standard CRT and MCRT in the presence of no, mild and severe scar, for different combinations of LV and RV pacing locations and delay intervals. Standard CRT caused a 21%, 23% and 21% change in dP/dt_{\max} from pacing combination D1-M2 5ms RVS, M3-P4 15ms RVA and M3-P4 45ms RVA for no scar, mild scar and severe scar, respectively. These changes correspond to an absolute increase of 0.150, 0.154 and 0.133 in the fraction of maximum dP/dt_{\max} reached for no scar, mild scar and severe scar cases, respectively. MCRT (2LV and 1RV stimulation sites) caused a 22%, 24% and 25% change in dP/dt_{\max} from pacing combination D1-M2 5ms M3-P4 5ms RVS, M3-P4 5ms D1-M2 5ms RVS M3-P4 5ms D1-M2 45ms RVS for no scar, mild scar and severe scar, respectively. These changes correspond to an absolute increase of 0.153, 0.164 and 0.162 in the fraction of maximum dP/dt_{\max} reached for no scar, mild scar and severe scar cases, respectively. Thus in the presence of severe scar there was a benefit with multisite vs conventional CRT (25% vs 21% representing a 19% relative improvement in the change in dP/dt_{\max}).

Figure 5 compares the optimal response from conventional CRT compared to multisite pacing.

CRT efficacy and QRS duration

To test if minimizing either biventricular or LV activation time is a potential method for optimising lead timings or positions, we plotted total and LV activation time against pacing efficacy in both the conventional and MCRT simulations in Figure 6.

Volume activation

Figure 7 plots the peak rate of volume activation (the rate of change of the fraction of the myocardial volume that is activated) for each pacing and scar combination, in the whole heart or only in the LV against the normalised dP/dt_{\max} .

LV Activation time

To evaluate the formation of continuous strands of activated tissue we calculated the time taken for short axis slices of the heart or the LV to become fully activated or the time taken for the first loop of continuous activation around the LV to form. Figure 8 shows the correlations between these times and dP/dt_{\max} .

Discussion

This is the first human biophysical model that has tested the efficacy of multisite LV pacing using a quadripolar lead. The model predicts that: 1) pre-excitation of the LV in regions of slow conduction improves hemodynamic response to CRT, 2) multisite CRT offers moderate improvements in acute hemodynamic response over conventional CRT but that this is the case only in the presence of scar 3) minimizing QRS duration or activation times of short

axis slices provide a poor indicator of CRT response and 4) cumulative volume activation maps provide a potential metric of CRT response that is robust to cases with scar.

Standard and MCRT

As shown in Figure 3 in the absence of scar approximately 0.85 of the maximum dP/dt_{\max} could be achieved with either standard or MCRT. It was only in the presence of postero-lateral scar that MCRT showed a benefit. As the level of scar increased the optimal response between multisite and standard CRT diverged (25% vs 21%, representing a relative increase of 19%). As the level of scar increased the optimal combination of poles locations in both the LV and RV changed for both standard and MCRT demonstrating the impact of scar on optimal lead placement.

Figure 3 shows that if the RV (apical or septal) is the first site to be activated then regardless of the severity of postero-lateral scar increasing the delay interval decreases CRT efficacy. In the presence of scar pre exciting the LV with standard CRT improves response, regardless of LV or RV pacing location, consistent with earlier studies which showed an improved benefit of LV pre-excitation over simultaneous LV and RV pacing (19; 20). Similarly for MCRT in the absence of postero-lateral scar the model predicts no significant benefit from LV pre excitation and limited benefit in the presence of mild scar for any pacing lead combination (Fig. 4). Only in the presence of severe scar was a benefit seen in pre exciting the LV for MCRT.

The effect of RV septal or apical pacing remains controversial (21; 22). In standard CRT RV septal pacing has been shown to provide no benefit over RV apical pacing (23). Consistent with these results the model predicted no clear benefit from RV septal or apical pacing for standard CRT. Interestingly, there was a consistently better response to CRT with RV septal pacing as opposed to apical pacing in the MCRT simulations.

Figure 3 and 4 predict that in a clinical context, when temporal optimisation may be unavailable or limited, MCRT provides an optimal or near optimal outcome in 85% of pacing combinations for near simultaneous activation compared to 71% of pacing combinations for conventional CRT. Meaning MCRT may provide a more robust outcome in the absence of temporal optimisation.

Pacing in Scar

Consistent with canine (24) and human (25) studies the model results predict that with optimal pacing timing and location, CRT in the presence of scar can still significantly improve pump function.

Specifically, the model predicts that, with lead capture, pacing in scarred regions and thus pre exciting the scarred myocardium often results in an optimal site. Controversy remains on the detrimental effects of pacing in or near scar (26–28), however, these conflicting results could be due to differences in capture of the scarred region, as if electrical activation fails to propagate from the pacing site then patients will receive no benefit. Notably lead position optimisation strategies have resulted in apparently conflicting conclusions. Previous reports have suggested that pacing in or near regions of scar compromises response (26; 27)

conversely an alternate strategy proposes pacing at the point of latest mechanical contraction maximises response (29–31). Although not explicitly inconsistent, in many cases slow conduction in scar will result in the last region to contract being one that is scarred or compromised, this location is then either an optimal or a poor pacing location depending on the doctrine adopted. The model predicts that if the scarred region has viable but slow conduction then pre-exciting the scarred region can result in an optimal response, thus the optimal increase in dP/dt_{max} for standard and MCRT was achieved by first pacing from D1 to M2 in the absence of scar, but in the presence of scar it was optimal to pace first from M3 to P4, which was located in the middle of the scar region. This is in keeping with non-contact mapping data from our institution where LV pre-excitation in areas of slow conduction improved hemodynamic response (32).

Apical vs basal pacing

There has been much interest recently in the position of the LV pacing lead for CRT in terms of an apical or basal pacing site. Recent data from the MADIT-CRT trial showed that leads placed in the apical region were associated with an unfavourable outcome (33). For standard CRT simulations, with a single LV stimulation site, the optimal site was basal in models with mild or severe scar. In models without scar there was marginal difference between apical and basal pacing. For MCRT, pacing at both apical and basal sites is performed so one cannot differentiate between apical and basal LV pacing. One potential advantage of this type of lead especially in patients with scar thus may be the ability to achieve a stable apical position within a CS branch and to perform basal stimulation using the proximal electrodes.

Optimising activation

Previous studies have reported that minimizing QRS correlates with CRT response (13; 34) whilst other studies found no change in QRS despite seeing a response to CRT (35; 36). To directly address this issue we evaluated the correlation between QRS duration, maximum rate of volume activation and short axis slice activation times in both the RV and LV and the LV alone. We found that QRS duration did not consistently correlate with CRT response. Single site LV pacing has been reported to prolong QRS while improving CRT response (18). This could be attributable to late activation of the RV prolonging the QRS while having limited impact on LV function, yet even when the confounding effects of the RV on total activation time were removed (Fig. 6) the correlation between CRT response and LV activation time in the model was still poor. This relationship was similar for both standard and MCRT with the relationship deteriorating further in the presence of scar.

We hypothesised that minimizing the activation time of the LV, RV and LV or a loop in a short axis slice would correlate with CRT response by corresponding to the formation of a continuous contracting region of myocardium that would cause an effective contraction of the LV. Despite showing a strong correlation of basal activation with CRT response in the absence of scar, this relationship deteriorated rapidly in the presence of scar, particularly in the MCRT simulations. It is possible that calculating the time of formation of other continuous loops of activating myocardium would correspond to CRT response. These loops could potentially lie out of the short axis plane or in loops of myocardium following the direction of principle stress.

The only metric to show a consistent correlation with the CRT response was the peak rate of cumulative activation in the LV. Given an approximate constant conduction velocity and the continuous smoothly varying LV geometry, this metric corresponds to the peak surface area of the activation wave and maximising its size will synchronise the bulk activation time of the heart. This metric correlated with both standard and MCRT and was independent of scar, RV or LV lead location and timing interval. The cumulative activation of the LV is not routinely measured in CRT patients. It can be approximated by evaluating the rate of cumulative volume contracting, although the relationship between activation time and deformation is dependent on the activation pattern. It is possible that simple patient specific activation models could provide a means to evaluate this metric and be used for the model guided optimisation of CRT lead position and timing.

Limitations

The model was based on a single patient dataset due to the need for a single comprehensive and consistent data set. However, we cannot necessarily assume that all patients would respond in the same fashion. The patient on whom the model was based, however, was a typical candidate for CRT with a broad left bundle branch block ECG and LVEF<35%.

In modelling the scar we assumed a homogenous and discrete region which may not be the case for many patients with ischemic heart disease that may have multiple and heterogeneous areas of scar. The presence of multiple infarct regions would affect the model predictions. Specifically, the presence of scarred or compromised regions in close proximity to the RV lead could favour pre excitation of the RV to achieve an optimal response. Late enhancement MRI shows us that scar geometry is varied and often complex. In this study we aimed to investigate the general impact of transmural postero lateral scar severity on conventional CRT and MCRT efficacy independently from any one individual patient's scar geometry. This led to the use of a defined analytical description of scar geometry, however, the model results may change for different scar locations or geometries.

Multisite pacing was delivered using a commercially available lead and it is possible that other lead designs would produce a different hemodynamic response.

Conclusions

This biophysical model, testing the efficacy of multisite LV pacing using a quadripolar lead, shows that MCRT may offer an improvement in acute hemodynamic response over conventional standard CRT but that this benefit is only seen in the presence of scar. Postero-lateral scar is a well recognized predictor of poor CRT response and therefore MCRT delivered using such lead technologies may be a potential way to improve response in the CRT population especially in patients with ischemic cardiomyopathy. These findings will clearly require in vivo evaluation.

Acknowledgements

This work was supported by United Kingdom Engineering and Physical Sciences Research Council for support through grants EP/F043929/1 and EP/F059361/1. The authors are grateful to Paul Ryu for Quartet lead technical specifications.

References

1. Cleland JGF, et al. The Effect of Cardiac Resynchronization on Morbidity and Mortality in Heart Failure. *ACC Current Journal Review*. 2005; 14:20–20.
2. Daubert C, et al. Prevention of Disease Progression by Cardiac Resynchronization Therapy in Patients With Asymptomatic or Mildly Symptomatic Left Ventricular Dysfunction: Insights From the European Cohort of the REVERSE (Resynchronization Reverses Remodeling in Systolic Left Ventricular Dysfunction) Trial. *J Am Coll Cardiol*. 2009; 54:1837–1846. [PubMed: 19800193]
3. Vardas PE, et al. Guidelines for cardiac pacing and cardiac resynchronization therapy. *European Heart Journal*. 2007; 28:2256–2295. [PubMed: 17726042]
4. Abraham WT, et al. Cardiac Resynchronization in Chronic Heart Failure. *NEJM*. 2002; 346:1845–1853. [PubMed: 12063368]
5. Leclercq C, et al. A Randomized Comparison of Triple-Site Versus Dual-Site Ventricular Stimulation in Patients With Congestive Heart Failure. *Journal of the American College of Cardiology*. 2008; 51:1455–1462. [PubMed: 18402900]
6. Forleo GB, et al. Left ventricular pacing with a new quadripolar transvenous lead for CRT: Early results of a prospective comparison with conventional implant outcomes. *Heart Rhythm*. 2011; 8:31–37. [PubMed: 20887804]
7. Shetty AK, et al. Use of a quadripolar left ventricular lead to achieve successful implantation in patients with previous failed attempts at cardiac resynchronization therapy. *Europace*. 2011; doi: 10.1093/europace/eur1032
8. Niederer SA, et al. Length-dependent tension in the failing heart and the efficacy of cardiac resynchronization therapy. *Cardiovascular Research*. 2011; 89:336–343. [PubMed: 20952413]
9. Plank G, et al. Algebraic Multigrid Preconditioner for the Cardiac Bidomain Model. *Biomedical Engineering, IEEE Transactions on*. 2007; 54:585–596.
10. Ursell P, et al. Structural and electrophysiological changes in the epicardial border zone of canine myocardial infarcts during infarct healing. *Circ Res*. 1985; 56:436–451. [PubMed: 3971515]
11. Rodriguez L-M, et al. Variable Patterns of Septal Activation in Patients with Left Bundle Branch Block and Heart Failure. *Journal of Cardiovascular Electrophysiology*. 2003; 14:135–141. [PubMed: 12693492]
12. Hodgkin AL. A note on conduction velocity. *The Journal of Physiology*. 1954; 125:221–224. [PubMed: 13192767]
13. Bax JJ, et al. Left ventricular dyssynchrony predicts response and prognosis after cardiac resynchronization therapy. *J Am Coll Cardiol*. 2004; 44:1834–1840. [PubMed: 15519016]
14. Lecoq G, et al. Clinical and electrocardiographic predictors of a positive response to cardiac resynchronization therapy in advanced heart failure. *European Heart Journal*. 2005; 26:1094–1100. [PubMed: 15728648]
15. Pitzalis MV, et al. Ventricular asynchrony predicts a better outcome in patients with chronic heart failure receiving cardiac resynchronization therapy. *Journal of the American College of Cardiology*. 2005; 45:65–69. [PubMed: 15629375]
16. Alonso C, et al. Electrocardiographic predictive factors of long-term clinical improvement with multisite biventricular pacing in advanced heart failure. *The American Journal of Cardiology*. 1999; 84:1417–1421. [PubMed: 10606115]
17. Yu C-M, et al. Predictors of left ventricular reverse remodeling after cardiac resynchronization therapy for heart failure secondary to idiopathic dilated or ischemic cardiomyopathy. *The American Journal of Cardiology*. 2003; 91:684–688. [PubMed: 12633798]
18. Leclercq C, et al. Systolic Improvement and Mechanical Resynchronization Does Not Require Electrical Synchrony in the Dilated Failing Heart With Left Bundle-Branch Block. *Circulation*. 2002; 106:1760–1763. [PubMed: 12356626]
19. Kurzidim K, et al. Invasive Optimization of Cardiac Resynchronization Therapy: Role of Sequential Biventricular and Left Ventricular Pacing. *Pacing and Clinical Electrophysiology*. 2005; 28:754–761. [PubMed: 16105000]

20. Sogaard P, et al. Sequential Versus Simultaneous Biventricular Resynchronization for Severe Heart Failure: Evaluation by Tissue Doppler Imaging. *Circulation*. 2002; 106:2078–2084. [PubMed: 12379577]
21. Mera F, et al. A Comparison of Ventricular Function During High Right Ventricular Septal and Apical Pacing after His-Bundle Ablation for Refractory Atrial Fibrillation. *Pacing and Clinical Electrophysiology*. 1999; 22:1234–1239. [PubMed: 10461302]
22. Victor F, et al. A Randomized Comparison of Permanent Septal Versus Apical Right Ventricular Pacing: Short-Term Results. *Journal of Cardiovascular Electrophysiology*. 2006; 17:238–242. [PubMed: 16643392]
23. Shimano M, et al. Does RV Lead Positioning Provide Additional Benefit to Cardiac Resynchronization Therapy in Patients with Advanced Heart Failure? *Pacing and Clinical Electrophysiology*. 2006; 29:1069–1074. [PubMed: 17038138]
24. Rademakers LMMD, et al. Myocardial Infarction Does Not Preclude Electrical and Hemodynamic Benefits of Cardiac Resynchronization Therapy in Dyssynchronous Canine Hearts. *Circulation: Arrhythmia and Electrophysiology*. 2010; 3:361–368. [PubMed: 20495014]
25. Jansen AHM, et al. The influence of myocardial scar and dyssynchrony on reverse remodeling in cardiac resynchronization therapy. *European Journal of Echocardiography*. 2008; 9:483–488. [PubMed: 17826355]
26. Bleeker GB, et al. Effect of Posterolateral Scar Tissue on Clinical and Echocardiographic Improvement After Cardiac Resynchronization Therapy. *Circulation*. 2006; 113:969–976. [PubMed: 16476852]
27. Ypenburg C, et al. Impact of viability and scar tissue on response to cardiac resynchronization therapy in ischaemic heart failure patients. *European Heart Journal*. 2007; 28:33–41. [PubMed: 17121757]
28. Riedlbauchová L, et al. The Impact of Myocardial Viability on the Clinical Outcome of Cardiac Resynchronization Therapy. *Journal of Cardiovascular Electrophysiology*. 2009; 20:50–57. [PubMed: 18803571]
29. Delgado V, et al. Relative Merits of Left Ventricular Dyssynchrony, Left Ventricular Lead Position, and Myocardial Scar to Predict Long-Term Survival of Ischemic Heart Failure Patients Undergoing Cardiac Resynchronization Therapy. *Circulation*. 123:70–78.
30. Ypenburg C, et al. Optimal Left Ventricular Lead Position Predicts Reverse Remodeling and Survival After Cardiac Resynchronization Therapy. *Journal of the American College of Cardiology*. 2008; 52:1402–1409. [PubMed: 18940531]
31. Khan FZ, et al. The Impact of the Right Ventricular Lead Position on Response to Cardiac Resynchronization Therapy. *Pacing and Clinical Electrophysiology*. 2011; 34:467–474. [PubMed: 21208234]
32. Lambiase PD, et al. Non-contact left ventricular endocardial mapping in cardiac resynchronisation therapy. *Heart*. 2004; 90:44–51. [PubMed: 14676240]
33. Singh JP, et al. Left Ventricular Lead Position and Clinical Outcome in the Multicenter Automatic Defibrillator Implantation Trial-Cardiac Resynchronization Therapy (MADIT-CRT) Trial. *Circulation*. 2011; 123:1159–1166. [PubMed: 21382893]
34. Molhoek SG, et al. QRS Duration and Shortening to Predict Clinical Response to Cardiac Resynchronization Therapy in Patients with End-Stage Heart Failure. *Pacing and Clinical Electrophysiology*. 2004; 27:308–313. [PubMed: 15009855]
35. Pitzalis MV, et al. Cardiac resynchronization therapy tailored by echocardiographic evaluation of ventricular asynchrony. *Journal of the American College of Cardiology*. 2002; 40:1615–1622. [PubMed: 12427414]
36. Yu C-M, et al. Comparison of Efficacy of Reverse Remodeling and Clinical Improvement for Relatively Narrow and Wide QRS Complexes After Cardiac Resynchronization Therapy for Heart Failure. *Journal of Cardiovascular Electrophysiology*. 2004; 15:1058–1065. [PubMed: 15363081]

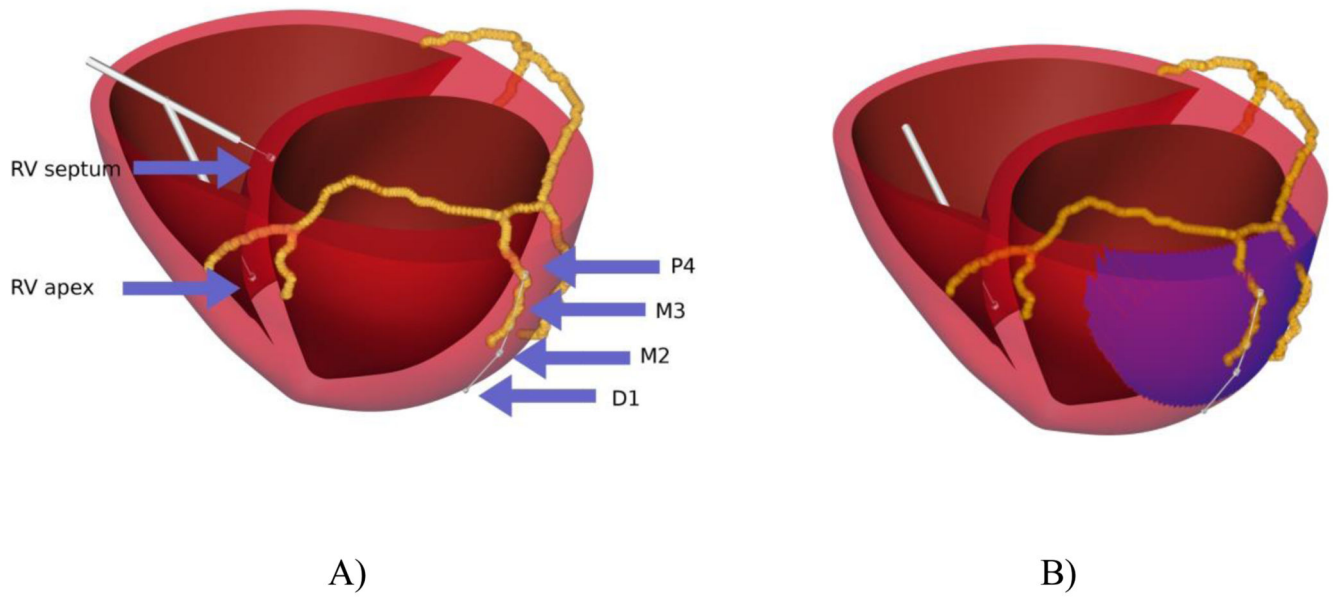


Figure 1. Heart geometry and coronary venous anatomy. Panel A) shows Electrode position and label and Figure B) shows the region LV postero-lateral scar in blue.

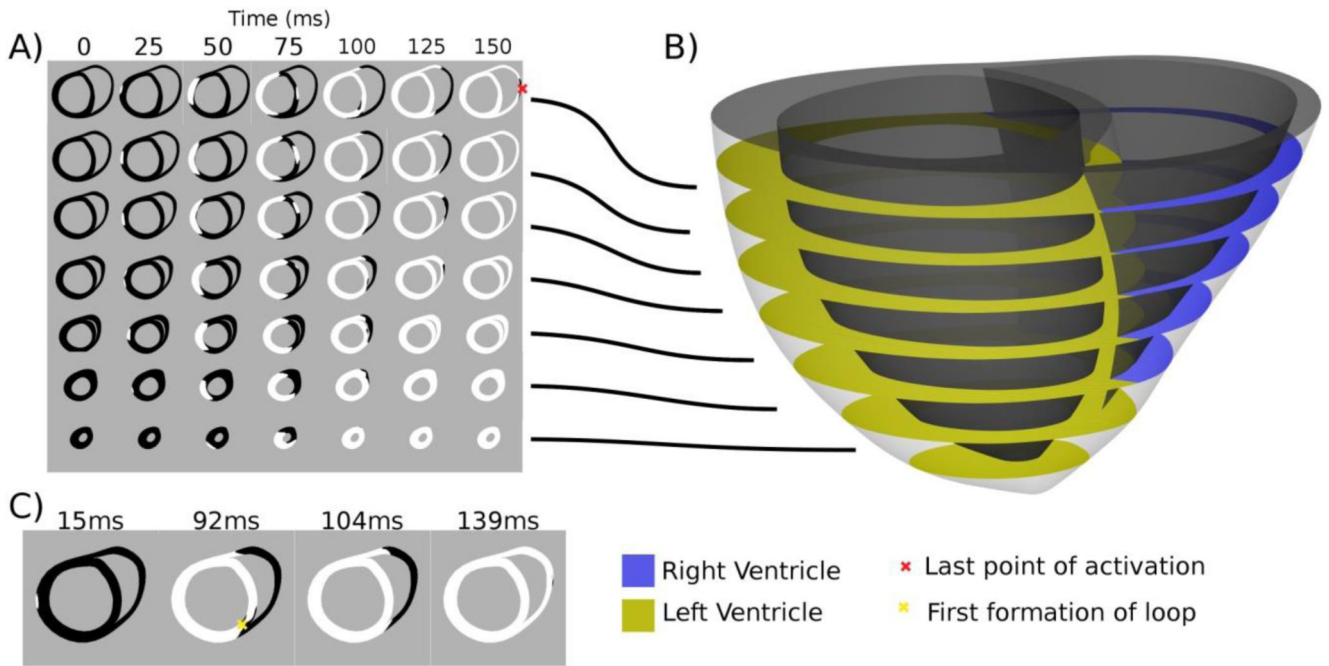


Figure 2.

Heart model activation cross sections. Panel A) shows the activation patterns, where white regions are activated and black regions inactivated for evenly spaced 10mm slices taken from the heart model in panel B). Panel C) shows the point of first activation at 15ms in slice 3, the point (marked with a yellow x) and time where the first loop of activation is formed at 92ms, the point when the LV is fully activated at 104ms and the time just prior to full slice activation at 139ms.

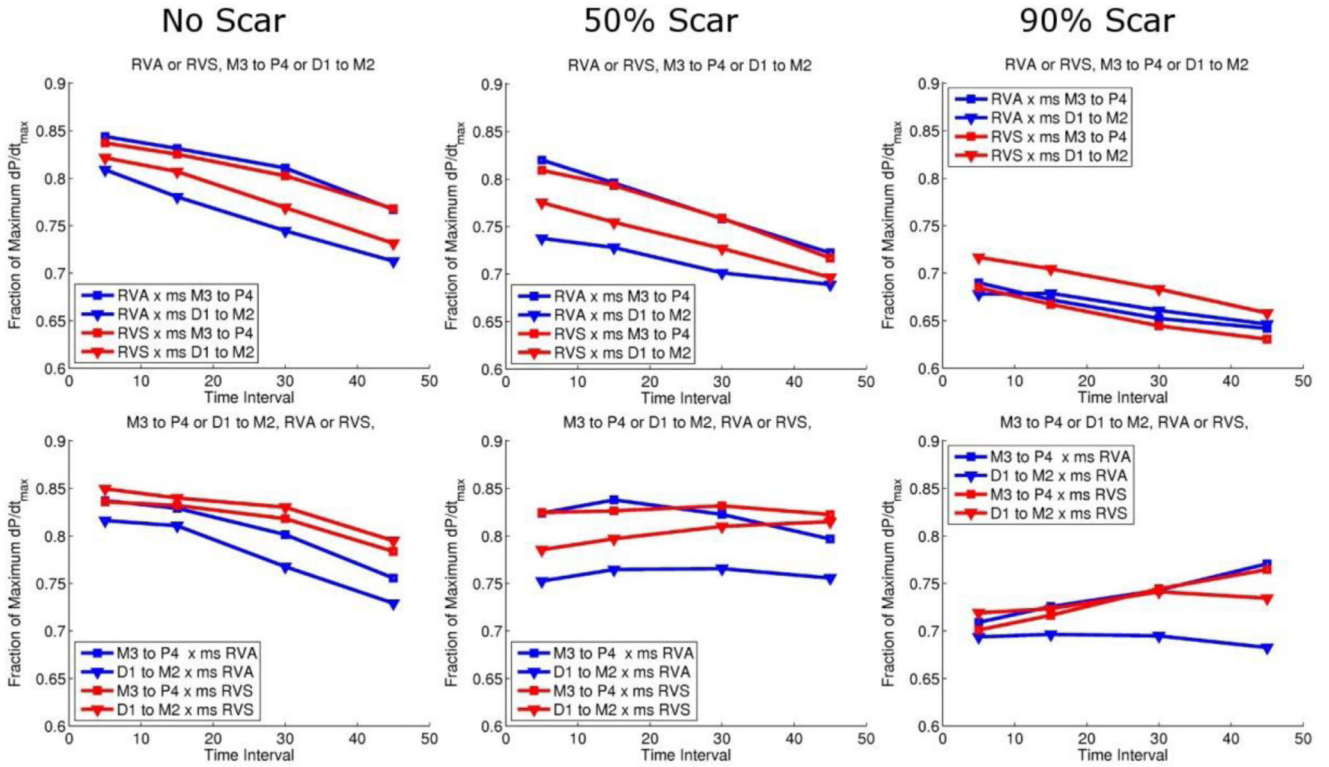


Figure 3. Standard CRT pacing response: top panel corresponds to pacing the RV first, and bottom panel pacing the LV first with increasing intervals between the two. Red lines correspond to septal and blue lines apical RV pacing. Triangle and squares symbols correspond to LV pacing from the apex or base, respectively.

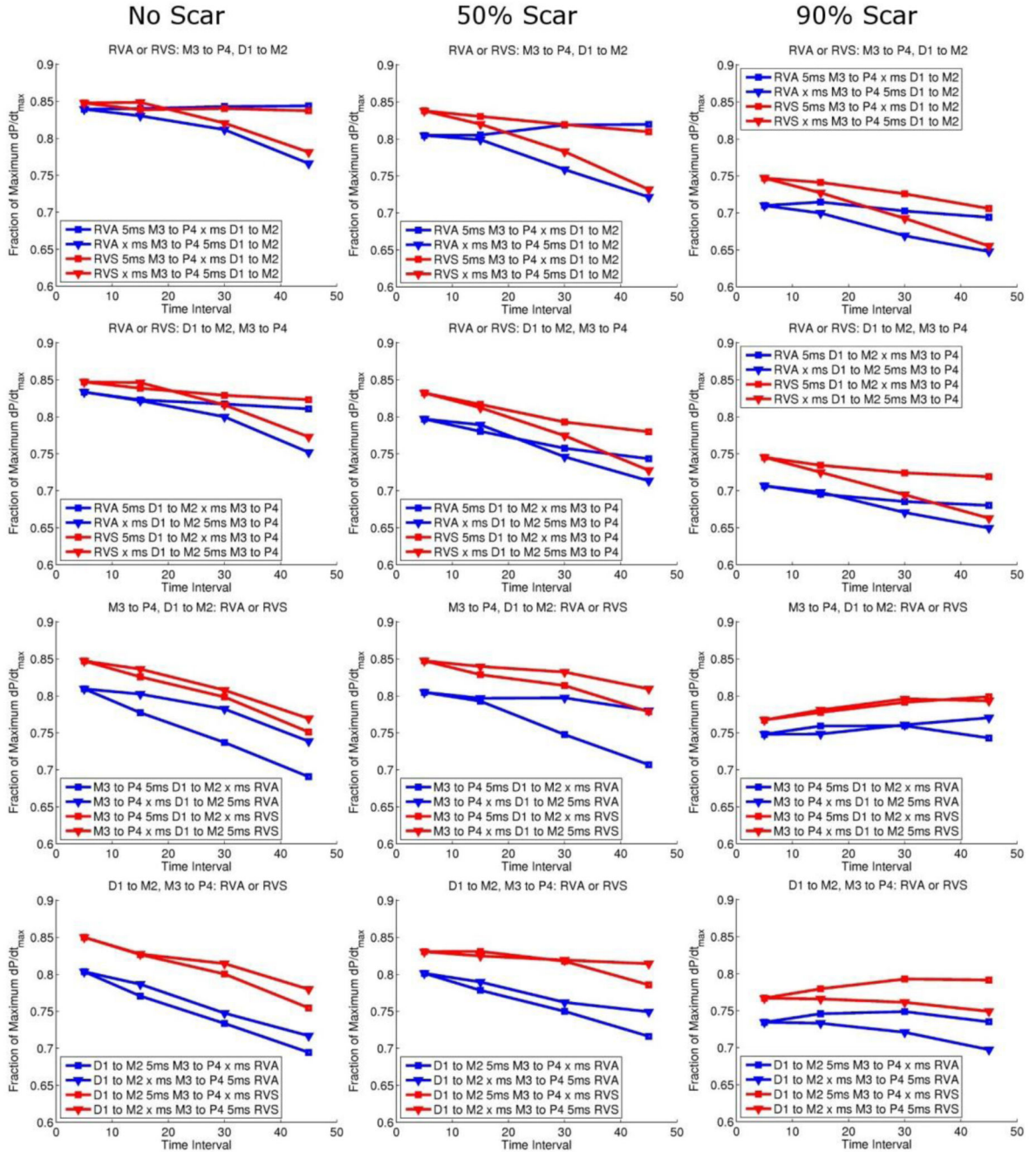
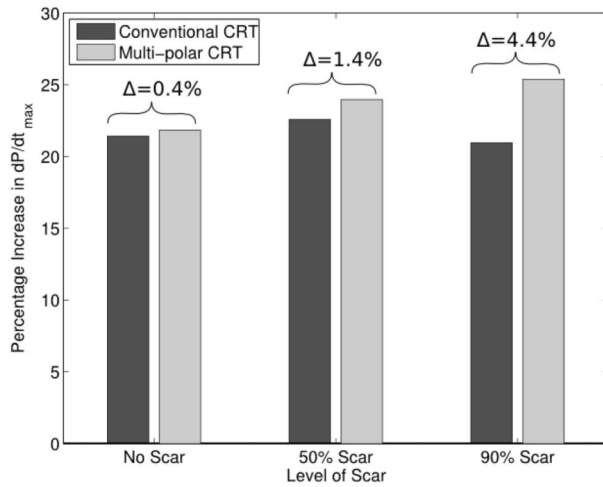
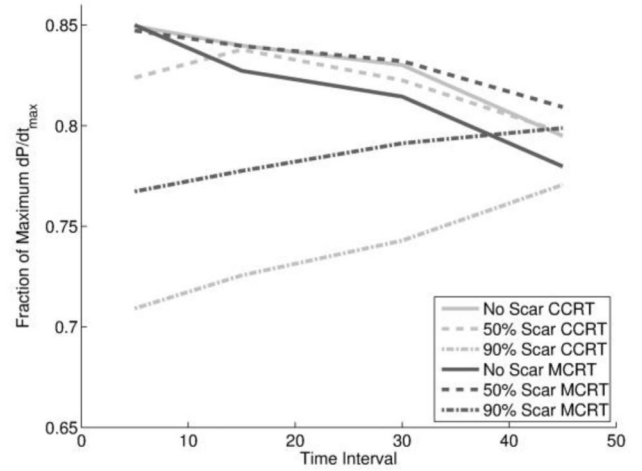


Figure 4. Multisite CRT pacing: red lines correspond to septal and blue apical RV pacing, and triangle and squares symbols correspond to the variable time interval being first or second, respectively.



A)



B)

Figure 5.

A) Hemodynamic effect of standard vs MCRT dependent on the presence and severity of postero-lateral scar. With difference between standard vs MCRT labelled. B) Comparison of optimal pacing combinations from Fig. 3 and 4, for conventional CRT (CCRT, grey lines) and Multi-polar CRT (MCRT, black lines) for no (solid line), 50% (dashed line) and 90% (dash dot line) scar.

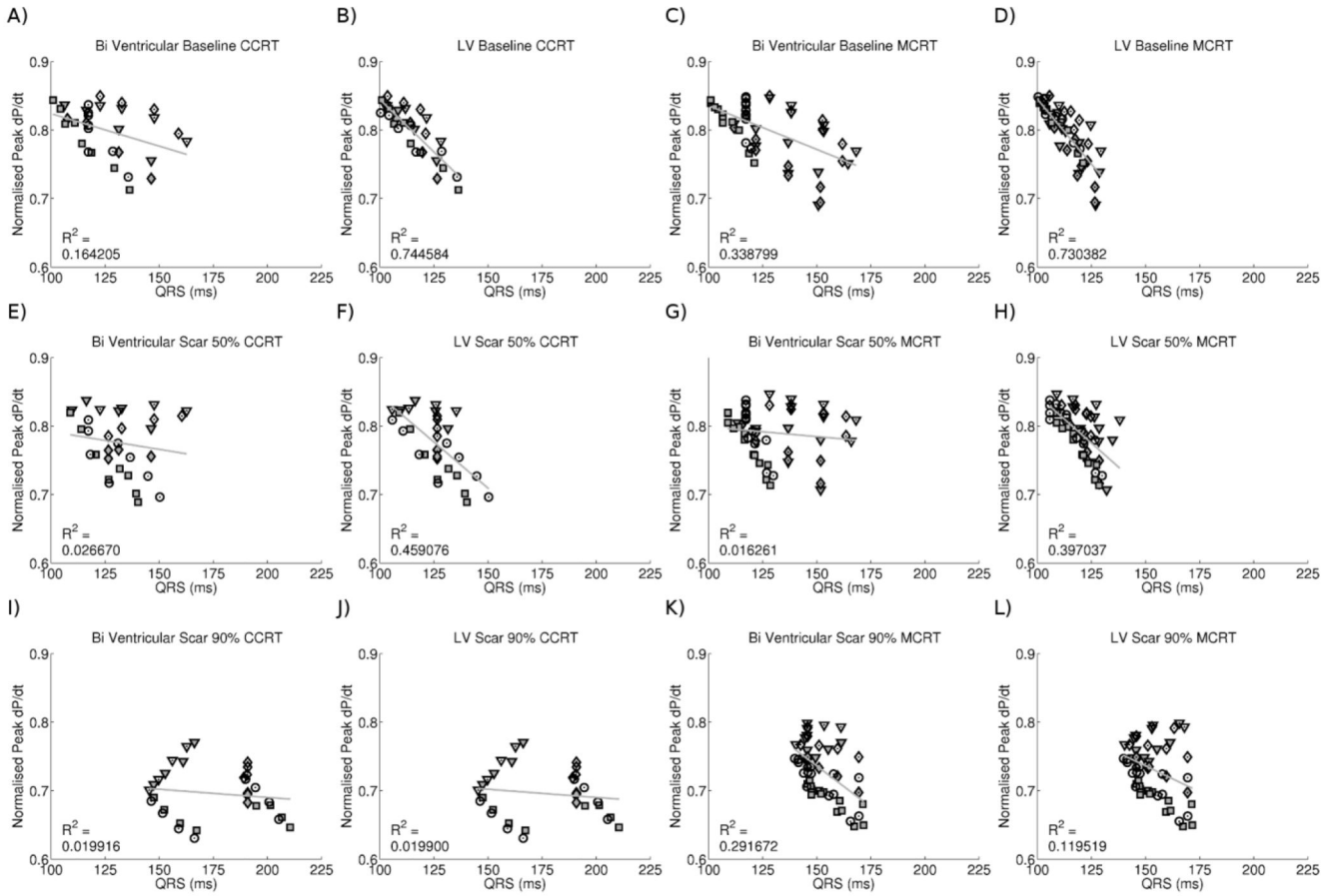


Figure 6.

Plot of normalised pressure against LV or biventricular activation time for conventional and MCRT in the presence of no, 50% and 90% scar. Point symbols correspond to pacing from RVA (square), RVS (circle), D1-M2 (triangle) or M3-P4 (diamond) first. Solid points correspond to RVA as opposed to RVS pacing.

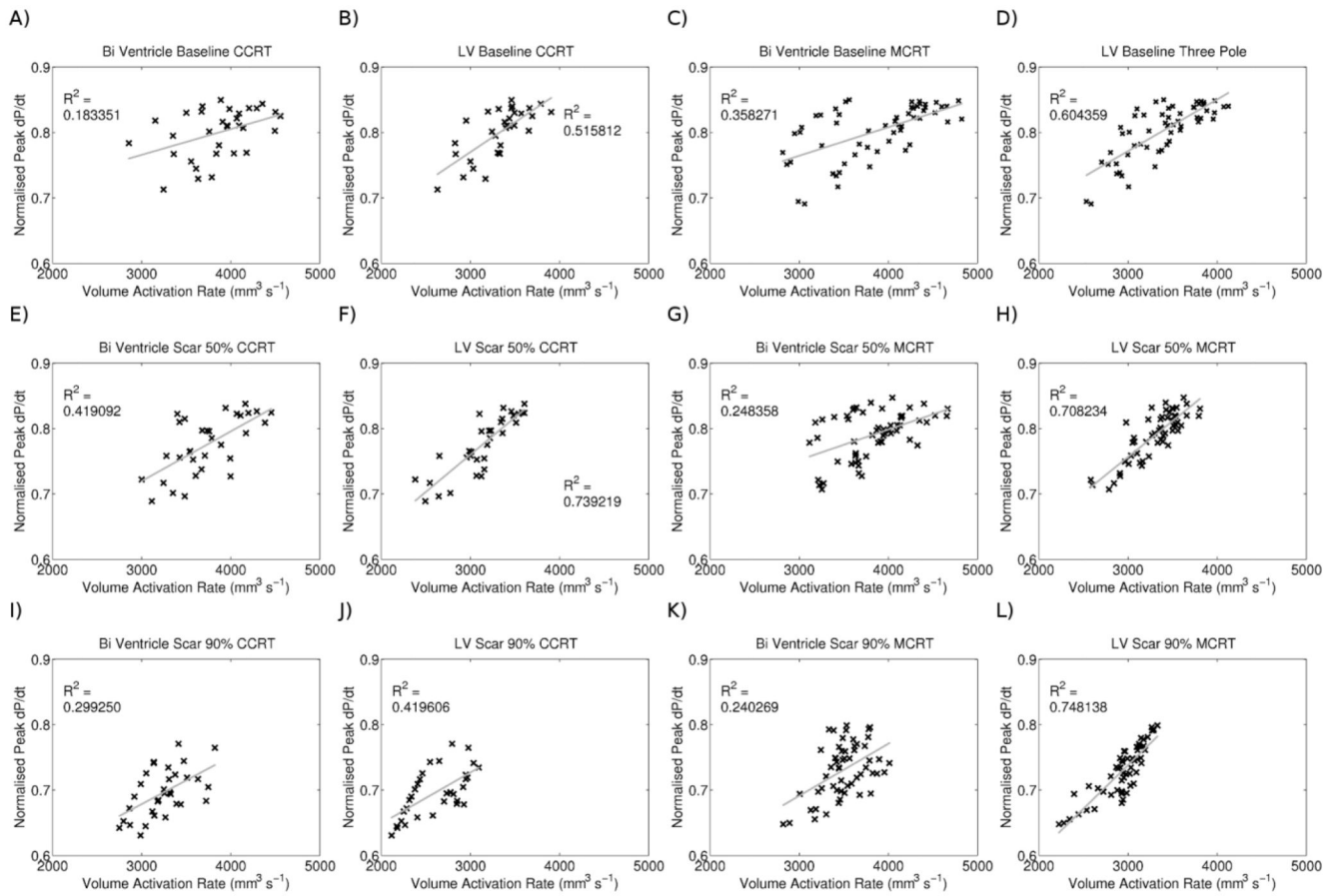


Figure 7. Correlation between CRT response and peak rate of cumulative activation for conventional CRT and MCRT in the presence of no, 50% and 90% scar.

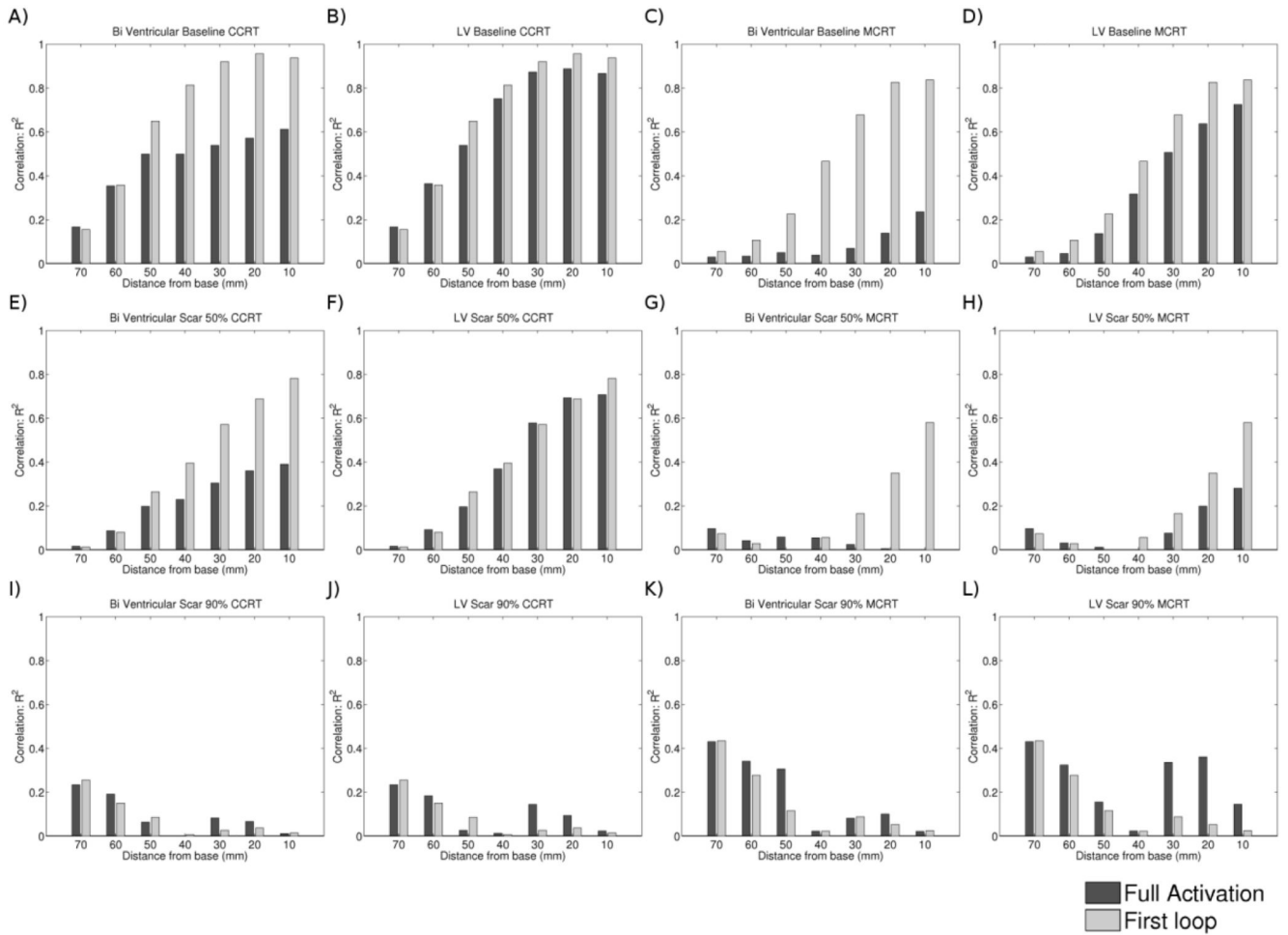


Figure 8. Correlation as defined by the R^2 value of a linear fit between the time taken for the whole slice or the first loop to form and the normalised rate of pressure development for conventional CRT (CCRT) and Multi-polar CRT (MCRT) with no, 50% scar and 90% scar.